The Influence of Motion Paths and Assembly Sequences on the Stability of Assemblies

Sourav Rakshit and Srinivas Akella, *Member, IEEE*

***Abstract*—In this paper, we present an approach for the stability analysis of mechanical part disassembly considering part motion in the presence of physical forces such as gravity and friction. Our approach uses linear complementarity to analyze stability as parts are moved out of the assembly. As each part is removed from the assembly along a specified path during disassembly, we compute the contact forces between parts in the remaining assembly; positive contact forces throughout the disassembly process imply the disassembly sequence is stable (since the parts remain in contact with one another). However, if the part that is being taken out induces motion of other parts in the remaining subassembly, we conclude the disassembly sequence is unstable. Thus, we are able to simulate the entire disassembly considering physical forces and part motion, which has not previously been done. We then show the influence of part motion on stable disassembly. In contrast to prior work on disassembly that has focused either on planning part motions based on only geometric constraints, or on analyzing the stability of an assembly without considering part motions, we explore the relation between part motion and the selection of stable disassembly sequences in 2-D and 3-D. We establish conditions that characterize path-dependent assemblies, where motion paths can play a significant role in stable disassembly. Since we track the motion of all parts in an assembly, instability inducing motions can be identified and prevented by introducing appropriate fixtures by selecting alternative disassembly sequences or by changing the motion paths. We extend the stability analysis for single part disassembly to stability analysis of subassembly disassembly. We additionally show that in the presence of friction, assembly and disassembly can be noninvertible.**

***Note to Practitioners*—Maintaining the stability of an assembly as assembly or disassembly proceeds is critical during product assembly, repair, and maintenance. While fixtures can ensure stability, they add cost and restrict access for parts and tools. We show that the stability of the assembly can depend on the paths taken by the parts, and present an approach for selecting paths that ensure stability from among the geometrically feasible paths. The main application is in assembly and disassembly planning for reducing the fixturing requirements and in planning assembly motions that do not cause instability. The results will also be useful in designing disassembly operations during maintenance or repair, when it may not be possible to fixture all parts. The stability analysis can also be used by assistive robots in domestic environments for tasks like stacking objects and for safe removal of collapsed structures after disasters such as earthquakes.**

***Index Terms*—Assembly planning, assembly sequence, motion path, stability analysis.**

Manuscript received November 28, 2013; revised April 11, 2014; accepted May 28, 2014. Date of publication August 21, 2014; date of current version April 03, 2015. This work was supported in part by the National Science Foundation under Awards CCF-0729161, IIS-1019160, and IIP-1266162. This paper was recommended for publication by Associate Editor T. D. Murphey and Editor J. Wen upon evaluation of the reviewers' comments. *(Corresponding author: Srinivas Akella.)*

S. Rakshit is with the Department of Mechanical Engineering, Indian Institute of Technology Madras, Chennai 600036, India (e-mail: srakshit@uncc.edu).

S. Akella is with the Department of Computer Science, University of North Carolina at Charlotte, Charlotte, NC 28223 USA (e-mail: s.akella@ieee.org).

Color versions of one or more of the figures in this paper are available online at http://ieeexplore.ieee.org.

Digital Object Identifier 10.1109/TASE.2014.2345569

I. Introduction

PRODUCT assembly is a labor-intensive and time-consuming process [35], [8]. Automated robotic assembly is aimed at reducing human cost and time. There has been significant research on several aspects of assembly automation including the development of algorithms for assembly sequencing considering part geometry [36], grasping of objects considering physical forces [21], [26], stability of subassemblies [23], [22], [24], and motion planning for part removal [32], [14], [19]. The simplest assembly problem is one in which there are only two hands, and the assembly sequence is monotone, i.e., each part is moved directly to its final position in the product without being placed in intermediate positions [36]. In this work, we consider monotone assembly of rigid parts using two hands. A classical strategy for assembly planning is assembly-by-disassembly [17]. This strategy is popular in assembly planning since a product in its assembled state has many more constraints than in its disassembled state; these constraints reduce the search space for a planner. When the parts are rigid and when only geometric constraints are considered, an inverted disassembly sequence leads to a feasible assembly sequence. Thus, the terms *assembly* and *disassembly* have been used interchangeably in the literature [36]. Note that disassembly by itself is important in repair, maintenance, and end-of-life processing [18].

We follow a simple definition of stability: A disassembly operation is said to be *stable*, if apart from the part(s) being removed, all other parts in the assembly stay in their respective locations. We make the initial assumption that a *stable* disassembly sequence when inverted will become a *stable* assembly sequence. In our work the fixed support is considered as a hand, so there is only one moving hand. The stability analysis we perform also has potential applications for robots in domestic environments, where tasks like stacking books, dishes, boxes, and even blocks (e.g., in the game Jenga [34]) are common. It may also be useful for autonomous construction and safe removal of collapsed structures during rescue operations after disasters such as earthquakes.

The focus of our work is the stability of the assembly in the presence of physical forces as each part is taken out of the assembly. We calculate the forces arising between the parts using

1545-5955 © 2014 IEEE. Personal use is permitted, but republication/redistribution requires IEEE permission.
See http://www.ieee.org/publications_standards/publications/rights/index.html for more information.

linear complementarity [2], [31]. The part motions are selected using the nondirectional blocking graph (NDBG) [36]. Our stability analysis is based on calculating the contact forces and identifying relative part motion. The initiation of breaking of contact in frictionless assemblies is reflected as a positive acceleration at the contact points, which is complementary to the contact force at those points. For assemblies with friction, the relative motion is indicated by the sliding velocity. We simulate the motion of part(s) during disassembly, calculate the contact forces and their complementary motions, and determine stability. Although the stability of assemblies has been analyzed previously [6], [23], [22], [24], and such analysis has been used to analyze the disassembly tree [25], the simulation of disassembly considering both physical forces and motion has not been previously addressed. Thus, our work can be incorporated into disassembly simulation and disassembly motion planning based on physical forces and constraints. Further, we demonstrate that the stability of disassembly sequences depends not only on the disassembly sequence, but also on the motion paths taken by the parts. We identify conditions that characterize such path-dependent assemblies. We show that for path-independent disassemblies, it is sufficient to perform stability analysis at only the nodes of the AND/OR assembly graph. We extend the stability analysis for single part disassembly to stability analysis of subassembly disassembly. Finally, we show that, in the presence of friction, assembly and disassembly can be noninvertible.

II. Related Work

There are two main areas of research related to our work: stability analysis and geometric analysis of assemblies. However, there has not been much prior work uniting these two areas for assembly planning.

A. Stability Analysis

Blum *et al.* [6] first analyzed the stability of rigid blocks. They defined an assembly of rigid blocks as stable if and only if all of the compressive contact forces between the blocks are positive and devised an algorithm similar to linear programming for solving the set of contact forces in the assembly. Palmer [27] investigated the computational complexity of stability of polygons and gave definitions of guaranteed stability, potential instability, and infinitesimal stability. Boneschanscher *et al.* [7] extended the linear programming-based approach of stability analysis to include insertion forces. Romney [30] presented a method for planar assemblies to concurrently generate both an assembly sequence and a fixture to hold intermediate subassemblies. In this sequence/fixture codesign problem, the fixtures must stabilize the (sub)assemblies against gravity and the insertion forces, while permitting insertion paths for the parts. Mattikalli *et al.* [23], [22] developed linear programming-based approaches for identifying the set of orientations under which an assembly is stable in the presence of gravity, both with and without friction. Mosemann *et al.* [24] developed a method similar to Mattikalli *et al.* and used it to analyze the stability of the subassemblies at each node of the AND/OR assembly graph [25]. Wolter and Trinkle [37] used a contact-force-based linear programming formulation to find optimal location of fixels in an assembly. Goldberg and Moradi [15] developed vertical assembly plans for assembly without fixtures, with a minimalist motivation similar to ours. With the exception of [25], very little work has used stability analysis systematically for the disassembly process. Moreover, it focuses mainly on the static analysis of the disassembly tree.

The notion of a stable equilibrium is closely related to force closure and form closure in robotic grasping [21], [26] and fixture design for a static assembly [9], [10]. Trinkle [33] formulated a first-order stability criterion for grasped objects based on linear programming. An assembly is *first-order stable* if all kinematically possible virtual displacements of the system result in a strict positive increase in potential energy of the system. First-order stability is equivalent to *robust directional equilibrium* for a system of rigid bodies and their fixtures, as formulated by Baraff *et al.* [3]. Our definition of stability is equivalent to *directional equilibrium* of Baraff *et al.* [3] and *weak stability* of Pang and Trinkle [28], which are defined to hold for an assembly if the contact forces that arise in response to an external force exactly balance the external force and induce zero body accelerations.

Stable transport of assemblies of parts without grasping has been studied by Bernheisel and Lynch [4], [5], who analyzed the stable transport of planar arrangements of parts by pushing motions. They identify force balance conditions that guarantee an assembly of parts stays assembled as it is pushed.

B. Geometric Analysis and Planning

For a concise overview of geometric assembly planning and sequencing, see [16]. The AND/OR graph representation of assembly sequences developed by de Mello and Sanderson [12] enables enumeration of all possible assembly sequences for automated planning. The nondirectional blocking graph (NDBG) is a subdivision of the space of all allowable motions of separation into a finite number of cells such that, within each cell, the set of blocking relations between all pairs of parts remains fixed [16]. The NDBG representation uses the geometry of the parts in the assembly to efficiently determine the set of feasible motion directions for a part, thus reducing the combinatorial complexity of disassembly sequencing [36]. The geometric information in the NDBG together with the sequencing information in an assembly AND/OR graph is then used to perform assembly sequencing. Halperin *et al.* [17] developed a motion space approach to generalize the NDBG to more general part motions.

More recently, disassembly planning has been addressed as a motion planning problem in the composite configuration space of the individual parts by applying sampling-based motion planners for planning part removal paths for disassembly [32]. Techniques have included sampling based on the geometry of reachable configurations. An RRT-based iterative planning approach that gradually decreases the allowed amount of interpenetration has been used for single part disassembly [14]. Le *et al.* [19] describe an RRT-based method for simultaneous disassembly sequencing and path planning; it can handle nonmonotone disassembly sequences. While these motion planners generate paths that avoid part interference, they do not consider any physical constraints such as gravity, friction, etc.

Portions of the work in this paper previously appeared in [29].

III. Problem and Approach

A. Motion Stability Problem

Given a geometrically feasible disassembly sequence and a motion path for an assembly, the *motion stability problem* is to identify whether the disassembly sequence and motion path are stable.

To solve the motion stability problem, we consider each part as it is removed from the assembly along a specified path and perform stability analysis to check whether the static equilibrium conditions are satisfied along the path for all parts of the assembly, other than the part being moved out. We declare a disassembly sequence and motion path to be *stable* when there is no relative motion between parts (excluding the part being moved by the gripper) along the path. Using this motion stability analysis, we can identify stable sequences and motion paths for disassembly from a given set of geometrically feasible disassembly sequences and motion paths for an assembly.

We make the following assumptions. We assume the assembly consists of polygonal parts (in 2-D) or polyhedral parts (in 3-D). We assume that each part that is moved out is held by a gripper. The moving part is assumed to undergo quasistatic motion with finite translations. There is perfect position control of the gripper and, hence, of the part that it grasps. The gripper does work only on the part that it holds and moves, except when moving a subassembly. The weight of the moving part is supported by the gripper, unless otherwise stated. When the gripper does not support the part, we assume it applies forces only along the motion path. Following the convention in the assembly planning literature, we do not consider collisions of the gripper with the assembly. We assume frictionless contact unless otherwise stated.

We use linear complementarity [11] to detect whether and when the assembly becomes unstable as each part is removed from the assembly. If linear complementarity finds a solution, i.e., all of the contact forces are non-negative and there is no relative motion between parts (excluding the part being moved by the gripper), then the assembly state is considered stable. The linear complementarity problem (LCP) proposed by Baraff [2] for analysis of frictionless cases calculates the relative movement in terms of the relative acceleration between the parts in the assembly. According to Baraff's model, for every contact point j in the assembly, the normal contact acceleration a_j and the normal contact force F_j form a complementary pair, i.e., $F_j \geq 0$, $a_j \geq 0$, and $F_j a_j = 0$. This statement, which implies that, when $F_j > 0$, $a_j = 0$, and when $a_j > 0$, $F_j = 0$, is represented succintly as $0 \leq F_j \perp a_j \geq 0$. We can sum up the complementarity conditions for all n contact points, and since a_j and F_j are linearly related [1], we have

$$\sum_{j=1}^{n} F_j a_j = \mathbf{F}^T \mathbf{a} = \mathbf{F}^T(\mathbf{A}\mathbf{F} + \mathbf{b}) = 0 \tag{1}$$

where $\mathbf{A} \in \mathbb{R}^{n \times n}$ is a positive semidefinite matrix. All external and body forces are grouped in the vector $\mathbf{b} \in \mathbb{R}^n$.

If friction is included, then, in addition to normal forces and accelerations, there will be a tangential component of force and acceleration at every contact point. When the static friction force limit is reached at any contact point, the matrix $\mathbf{A}$ is no longer positive semidefinite. Baraff's method cannot solve problems when $\mathbf{A}$ is not positive semidefinite. The Stewart–Trinkle model [31] gives a complementarity formulation for multibody contact problems with dynamic friction that can be solved using Lemke's algorithm [11]. Hence, we use the Stewart–Trinkle model for disassembly problems with friction. In the Stewart–Trinkle model, at each contact point j, the complementary constraints are

$$0 \leq d_{n_j} \perp p_{n_j} \geq 0 \tag{2}$$

$$0 \leq \boldsymbol{\rho}_j = \lambda_j \mathbf{e}_j + \mathbf{W}_{f_j}^T \mathbf{v} \perp \mathbf{p}_{f_j} \geq \mathbf{0} \tag{3}$$

$$0 \leq \zeta_j = \mu p_{n_j} - \mathbf{e}_j^T \mathbf{p}_{f_j} \perp \lambda_j \geq 0 \tag{4}$$

where d_{n_j} is the normal distance between the two parts at j, p_{n_j} is the normal component of the contact impulse, $\mathbf{p}_{f_j}$ is the friction component of the contact impulse, $\mathbf{e}_j \in \mathbb{R}^D$ is a vector of ones, D is the number of edges of the friction pyramid, λ_j is a variable that approximates the magnitude of the sliding velocity, μ is the Coulomb friction coefficient, n_d is the dimension of the configuration space, and $\mathbf{W}_{f_j} \in \mathbb{R}^{n_d \times D}$ is the friction contact wrench matrix that transforms the generalized velocity $\mathbf{v} \in \mathbb{R}^{n_d}$ of the part along the tangential component of the friction cone. For a two-dimensional problem ($n_d = 3$), at each contact point j, there are only two directions $\{\mathbf{t}_j, -\mathbf{t}_j\}$ of the friction component of the contact impulse, each perpendicular to the outward contact normal $\mathbf{c}_{n_j}$. The friction contact wrench matrix $\mathbf{W}_{f_j}$ is $\begin{bmatrix} \mathbf{t}_j & -\mathbf{t}_j \\ \mathbf{r}_j \otimes \mathbf{t}_j & -\mathbf{r}_j \otimes \mathbf{t}_j \end{bmatrix}$, where $\mathbf{r}_j$ is the vector from the part centroid to contact point j, and $\otimes$ is the 2-D equivalent of cross-product.

Using the Stewart–Trinkle model, we formulate the motion path stability problem as a linear complementarity problem as follows:

$$\begin{aligned} 0 \leq & \begin{bmatrix} \tilde{\mathbf{A}}_{nn} & \tilde{\mathbf{A}}_{nf} & \mathbf{0} \\ \tilde{\mathbf{A}}_{fn} & \tilde{\mathbf{A}}_{ff} & \tilde{\mathbf{E}} \\ \tilde{\boldsymbol{\mu}} & -\tilde{\mathbf{E}}^T & \mathbf{0} \end{bmatrix} \begin{bmatrix} \tilde{\mathbf{p}}_n^t \\ \tilde{\mathbf{p}}_f^t \\ \tilde{\boldsymbol{\lambda}}^t \end{bmatrix} + \begin{bmatrix} \tilde{\mathbf{b}}_n^t \\ \tilde{\mathbf{b}}_f^t \\ \mathbf{0} \end{bmatrix} \\ = & \begin{bmatrix} \frac{\tilde{\mathbf{d}}_n^t}{\Delta t} \\ \tilde{\boldsymbol{\rho}}^t \\ \tilde{\boldsymbol{\zeta}}^t \end{bmatrix} \perp \begin{bmatrix} \tilde{\mathbf{p}}_n^t \\ \tilde{\mathbf{p}}_f^t \\ \tilde{\boldsymbol{\lambda}}^t \end{bmatrix} \geq 0 \end{aligned} \tag{5}$$

where superscript t indicates value at time t. $\tilde{\mathbf{p}}_n = [p_{n_1}, \ldots, p_{n_K}]^T$, $\tilde{\mathbf{p}}_f = [\mathbf{p}_{f_1}, \ldots, \mathbf{p}_{f_K}]^T$, and $\tilde{\boldsymbol{\lambda}} = [\lambda_1, \ldots, \lambda_K]^T$ are the concatenated normal contact impulses, friction impulses, and λs, respectively, for all of the K contact points in the assembly, and $\tilde{\mathbf{A}}_{nn} = \tilde{\mathbf{W}}_n^T \tilde{\mathbf{M}}^{-1} \tilde{\mathbf{W}}_n$, $\tilde{\mathbf{A}}_{nf} = \tilde{\mathbf{W}}_n^T \tilde{\mathbf{M}}^{-1} \tilde{\mathbf{W}}_f$, $\tilde{\mathbf{A}}_{ff} = \tilde{\mathbf{W}}_f^T \tilde{\mathbf{M}}^{-1} \tilde{\mathbf{W}}_f$, $\tilde{\mathbf{A}}_{fn} = \tilde{\mathbf{W}}_f^T \tilde{\mathbf{M}}^{-1} \tilde{\mathbf{W}}_n$, $\tilde{\mathbf{b}}_f = \tilde{\mathbf{W}}_f^T \tilde{\mathbf{M}}^{-1} \left(\tilde{\mathbf{F}}_b + \tilde{\mathbf{F}}_{ext} \right) \Delta t$ and $\tilde{\mathbf{b}}_n = \tilde{\mathbf{W}}_n^T \left(\tilde{\mathbf{M}}^{-1} \left(\tilde{\mathbf{F}}_b + \tilde{\mathbf{F}}_{ext} \right) \Delta t + \tilde{\mathbf{v}}^{t-1} \right) + \tilde{\mathbf{d}}_n^{t-1} / \Delta t$.

$\tilde{\mathbf{M}}$ is the concatenated mass matrix, $\tilde{\mathbf{W}}_n = [\mathbf{W}_{n_1}, \ldots, \mathbf{W}_{n_K}]$ is the concatenated normal contact wrench matrix where $\mathbf{W}_{n_j}^T = \begin{bmatrix} \mathbf{c}_{n_j} & \mathbf{r}_j \otimes \mathbf{c}_{n_j} \end{bmatrix}$, $\tilde{\mathbf{W}}_f = [\mathbf{W}_{f_1}, \ldots, \mathbf{W}_{f_K}]$ is the concatenated friction wrench matrix, $\tilde{\boldsymbol{\mu}} = diag[\mu_1, \ldots, \mu_K]$, $\tilde{\mathbf{E}} = diag[\mathbf{e}_1, \ldots, \mathbf{e}_K]$, $\tilde{\mathbf{d}}_n = [d_{n_1}, \ldots, d_{n_K}]^T$, $\tilde{\boldsymbol{\rho}} = [\boldsymbol{\rho}_1, \ldots, \boldsymbol{\rho}_K]^T$, $\tilde{\boldsymbol{\zeta}} = [\zeta_1, \ldots, \zeta_K]^T$, $\tilde{\mathbf{v}}^t$ is the concatenated generalized velocity at time t, and $\tilde{\mathbf{F}}_b$

and $\tilde{\mathbf{F}}_{ext}$ are the concatenated body and external forces for all of the parts.

After each time step Δt, we update the position of the moving part, and then use linear complementarity [(1) or (5)] to calculate the contact forces and any relative motion (acceleration or sliding velocity) of the parts in the assembly. Tangential accelerations need to be checked for only those bodies in the assembly that can move according to the NDBG of the assembly, ignoring bodies that are blocked in the tangential direction. After obtaining the contact forces, we can check the existence of tangential acceleration in a body by calculating the net force in the tangential direction.

B. Simulation and Stability Analysis of Disassembly

We now describe the algorithm to perform stability analysis at each stage of disassembly; it uses linear complementarity for contact force computation, and a path planner to identify motion paths for the parts that are consistent with the NDBG. We describe the approach for evaluating a disassembly sequence for an assembly (see Algorithm 1).

Let $A_N(\bar{q}_N)$ be a complete assembly of N parts with configuration $\bar{q}_N$, $S = \langle P_1, P_2, \ldots, P_N \rangle$ be a disassembly sequence with parts numbered in their disassembly order, and $A_{N-i}(\bar{q}_{N-i})$ be the remaining assembly after the first i parts of the sequence have been removed. Given part P_{i+1} at its current configuration q, the function MotionPath returns a geometrically feasible path $\langle \hat{d} \rangle$ as a sequence of equal magnitude displacement vectors $\hat{d}_k$ for P_{i+1} to move out of $A_{N-i}(\bar{q}_{N-i})$. Each motion step $\hat{d}_k \in \langle \hat{d} \rangle$ is executed and the part P_{i+1} is moved for time Δt with a unit velocity along $\hat{d}_k$. After P_{i+1} has moved to its updated position q, the function LCPsolve $(A_{N-i}(\bar{q}_{N-i}), P_{i+1}(q))$ is called to solve the LCP problem of (1) (for the frictionless case) or (5) (for the friction case) and compute the contact forces. LCPsolve returns *true* (i.e., stable) if none of the contact relative motions (accelerations for the frictionless case and velocities for the friction case) are greater than zero. If any of the contact relative motions are greater than zero, LCPsolve returns *false* (i.e., unstable) and the simulation is terminated.

Algorithm 1 Stability Analysis of a Disassembly Sequence

Input: Assembly A_N, Disassembly Sequence $S = \langle P_1, \ldots, P_N \rangle$

1: **for** $i = 0, \ldots, N-1$ **do**
  2: $\langle \hat{d} \rangle = \text{MotionPath}(A_{N-i}(\bar{q}_{N-i}), P_{i+1}(q))$
  3: **if** $\langle \hat{d} \rangle == \emptyset$ **then**
    4: **return** GEOMETRICALLY INFEASIBLE
  5: **end if**
  6: **for** $k = 1, \ldots, \text{length}(\langle \hat{d} \rangle)$ **do**
    7: $v_{gripper} = \hat{d}_k / \|\hat{d}_k\|$
    8: $q \leftarrow q + v_{gripper} \cdot \Delta t$
    9: Stableflag $= \text{LCPsolve}(A_{N-i}(\bar{q}_{N-i}), P_{i+1}(q))$
    10: **if** Stableflag $==$ FALSE **then**
      11: **return** UNSTABLE
    12: **end if**
  13: **end for**
14: **end for**
15: **return** STABLE

IV. Examples

We now present a few examples to illustrate the approach. For a specified disassembly sequence, the parts in the assembly are moved along motion paths with directions consistent with the NDBG. At each time step, we calculate the contact forces between different bodies by linear complementarity. If at any time during the simulation, the part that is being moved out by the gripper induces a relative motion at any contact point in the rest of the assembly, we conclude that the assembly is unstable. Unless otherwise stated the gravitational acceleration g is assumed to be unity, mass density of the blocks is unity, and the simulation time step is 1 second. We will refer to a point i as *vertex* i if it is a vertex of the body or as a *contact point* i if it is the corresponding point on the mating body. We will depict the block moved by the gripper in red in the figures. For stability analysis, we use our MATLAB implementation of Baraff's complementarity algorithm for the frictionless case, unless otherwise stated, and for the case with friction, we use a MATLAB interface to the LCPPATH solver [13].

A. Simple Example With Blocks

This example (Fig. 1) has a set of frictionless blocks arranged such that if block C is lifted before block D, block B topples. We use Baraff's complementarity method to analyze this. Consider the disassembly sequence C-D-B-A, with vertical motion of C (any direction in the upper halfplane above B is permitted by the NDBG). As C is lifted up, we plot the contact forces, normalized with respect to the weight of moving block C, in Fig. 2. At 0 s, all the contact forces are positive. However, at 1 s, when block C is detached from the rest of the assembly, acceleration at contact point 4 is positive indicating that the rest of the assembly has become unstable. A similar situation occurs when block C is moved horizontally to the left or right. Thus, all disassembly sequences starting with the removal of block C are unstable.

By similar analyses, we can show that all disassembly sequences that start with the removal of blocks A, B, or C are unstable. Now consider the sequence D-C-B-A. We show the contact forces (normalized with respect to the weight of the block B) in Fig. 3. As each block is lifted up vertically, the contact forces for that particular block become zero. However all other contact forces are positive indicating the remaining subassemblies in all cases are stable. From the complementarity formulation, this implies that the contact accelerations are zero, i.e., none of the contacts are breaking. Hence, D-C-B-A is a stable

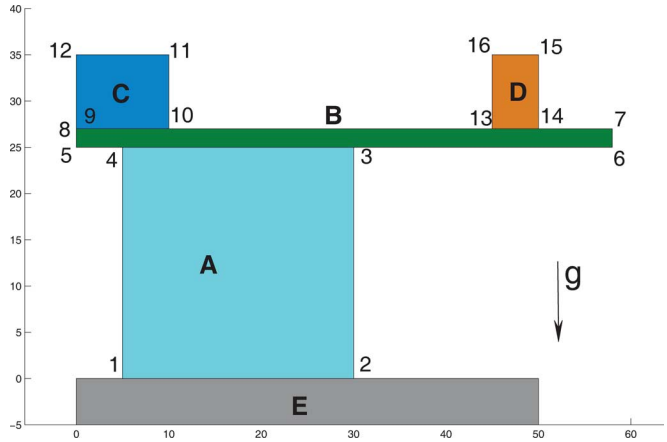

Fig. 1. Simple blocks example: an arrangement of blocks in an equilibrium configuration. The blocks are identified by alphabets and vertices by numbers. Block E is the fixed table. Based on [6].

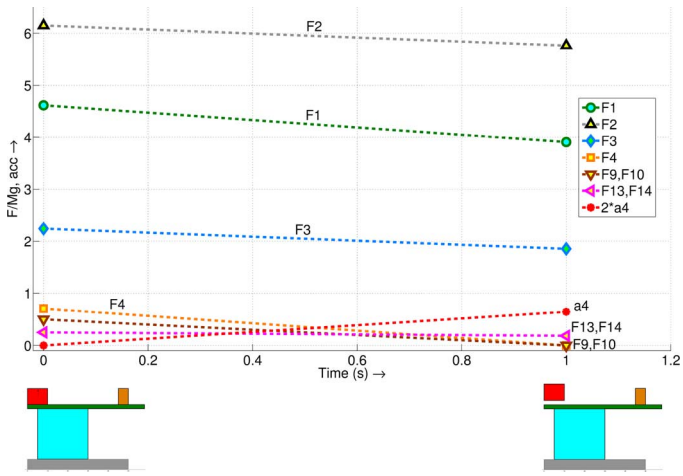

Fig. 2. Plot of contact forces (normalized by weight of the moving block C) against time as block C is lifted up. As soon as C is lifted up, contact point 4 has positive acceleration indicating that the remaining assembly is unstable.

disassembly sequence and is in fact the only stable disassembly sequence.

B. Example: Stable Disassembly With and Without Fixels

When disassembly sequences selected using only geometric constraints lead to instability, we can use fixels (i.e., point fixtures) to constrain parts that become unstable as other parts are removed. Using stability analysis, the parts that become unstable at the time of removal of other parts can be identified and stabilized by fixels or alternative disassembly sequences can be generated.

This example illustrates the use of fixels in maintaining stability of an assembly. Consider blocks A, B, and C on table D (Fig. 4). Only block A can move vertically up according to the NDBG. However, as soon as A is lifted up, B becomes unstable [Fig. 5(a)], with rightward accelerations of vertices 9 and 12. The instability in B when A is moved out can be prevented by application of fixels at appropriate locations on B [Fig. 5(b)]. Fixel positioning can be optimized using existing methods, e.g., [37].

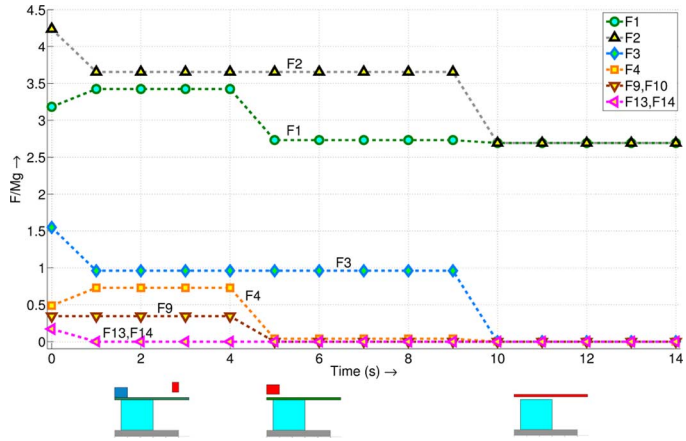

Fig. 3. Plot of contact forces for disassembly sequence D-C-B-A. X-axis is time, Y-axis is contact force normalized by the weight of block B. The forces at the contact points of each block remain positive until that block is lifted. This implies that the disassembly sequence is stable.

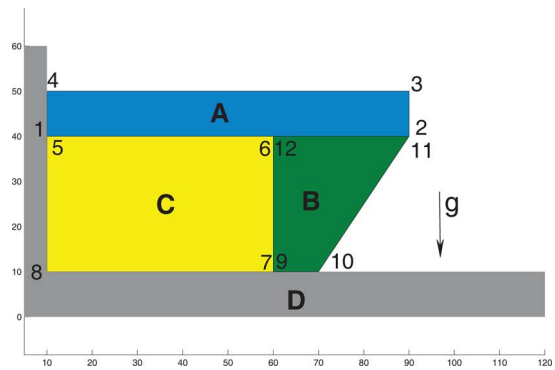

Fig. 4. Blocks A, B, and C rest on a frictionless base D.

V. Effect of Motion Paths on Stability

We now examine the question: Are part motion paths important during disassembly and assembly? The stability analysis that we have presented so far can alternatively be performed by analyzing the stability of the subassemblies at each node of the assembly sequence AND/OR graph, as in Mosemann *et al.* [25]. In our work, we simulate the process of disassembly by considering part motion. We next demonstrate that motion paths are *also* important for determining stable disassembly sequences. We show that instability can occur not only due to the order in which parts are removed, but also due to the motion paths by which they are removed.

We will call the class of problems where stable disassembly depends on motion paths *path-dependent disassembly* problems. The complementary class of stable disassembly problems where motion paths do not affect stability will be referred to as *path-independent disassembly* problems. Next we present both 2D and 3D examples to illustrate how stable disassembly depends on the choice of the motion path.

A. Influence of Motion Path in 2D

Consider the task of disassembling blocks A, B, C, and D from the part E on a fixed table (Fig. 6). This example, where the blocks are constrained to move through the exits I–V in Fig. 6, illustrates the effect of motion paths on stability. A and B can

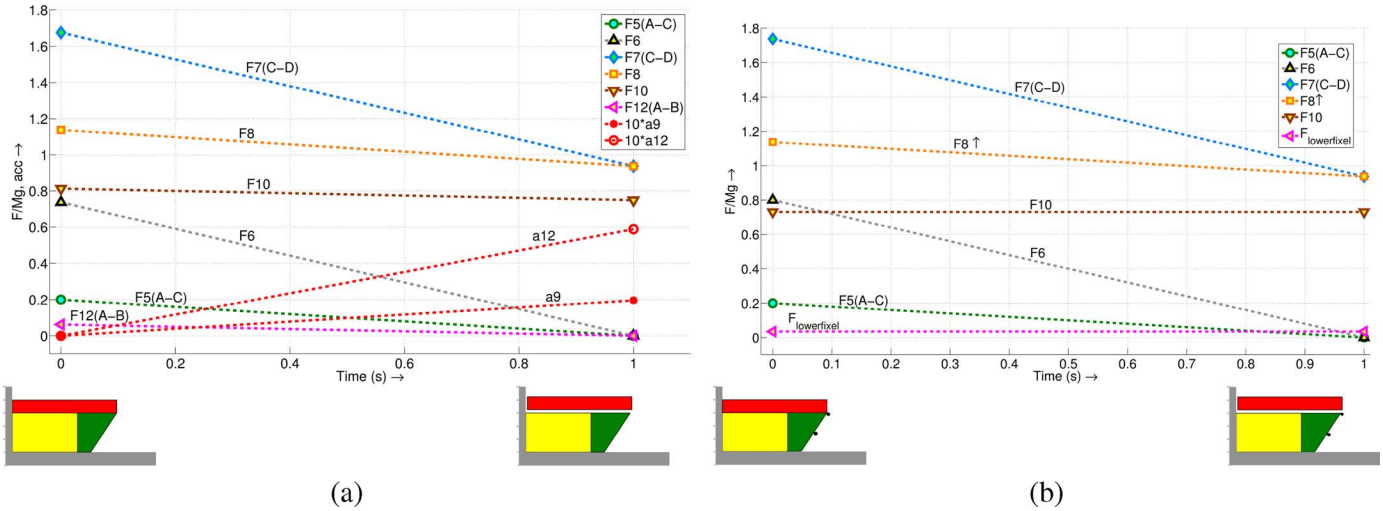

Fig. 5. Plot of contact forces as block A is lifted up vertically. X-axis is time, Y-axis is contact force normalized by the weight of the moving block A. Note that since there can be more than one normal at a contact vertex, we indicate the bodies between which the contact forces act in the legend of forces and accelerations. (a) Without fixels: as soon as block A is lifted, block B becomes unstable. This is indicated by positive accelerations at vertices 9 and 12 (scaled by a factor of 10 and shown in red). (b) With fixels: since the preceding analysis indicates that B loses contact in the horizontal right direction, we put fixels on the right hand free face of B at vertex 11 and midway between vertices 11 and 10 (as shown in the bottom figures). Now, when A is lifted up, B stays in position, and none of the contact vertices have positive accelerations.

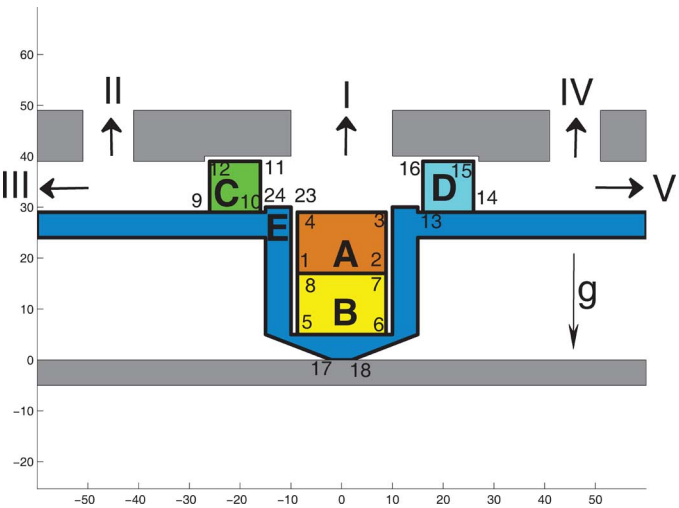

Fig. 6. Example to illustrate the effect of motion paths on stability. A, B, C, and D are movable frictionless blocks resting on a nonfixed body E that rests on a table (colored grey). The exits are numbered using Roman numerals.

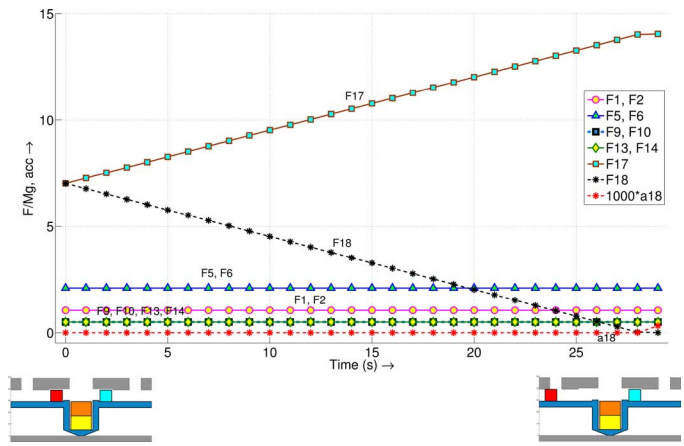

Fig. 7. Plot of contact force normalized with respect to the weight of C, and acceleration versus time. When C is moved to the left and lifted up to exit through II at 25 s, no instability is induced. However, when block C is moved to the extreme left towards exit III, at 29 s, the rest of the assembly becomes unstable, as indicated by positive acceleration at vertex 18.

move out through exit I, whereas C and D can move out through exits I–V. The shoulders on the rim of the cavity holding A and B prevent C and D from contacting A when exiting through I. All of the blocks are frictionless. The weight of the moving part is not supported by the gripper unless the part itself becomes unstable.

Since this example is symmetric about the vertical axis, we analyze the effect of the motion of block C to illustrate the influence of motion paths (i.e., choice of exits) on the stability of the assembly. C has geometrically feasible paths out of the assembly through any of its three nearest exits I, II, and III.

We first illustrate the influence of motion paths on stability. Consider the removal of C through exit III. As C is moved to the left through the passage leading to exits II and III, the contact force at vertex 17 increases and that at 18 decreases (Fig. 7) to counterbalance the increasing moment produced by the weight of C. At 25 s, when C is directly below exit II, it can be moved up towards exit II without instability. However, at 29 s, when C is at exit III, the assembly becomes unstable. This is indicated by positive acceleration at vertex 18.

When C is lifted up and moved towards exit I, no instability is induced in the assembly. Hence, for disassembly sequences that begin with the removal of C, the first step in the disassembly sequence is stable when C exits through I and II, and not through exit III. A similar situation occurs with D.

Next, we illustrate the interplay of motion paths and assembly sequences in maintaining stability. Consider removal of A first, followed by C. At 25 s, when C is positioned to exit through II [Fig. 8(a)], the assembly becomes unstable due to positive acceleration at vertex 18. Hence C cannot exit either through

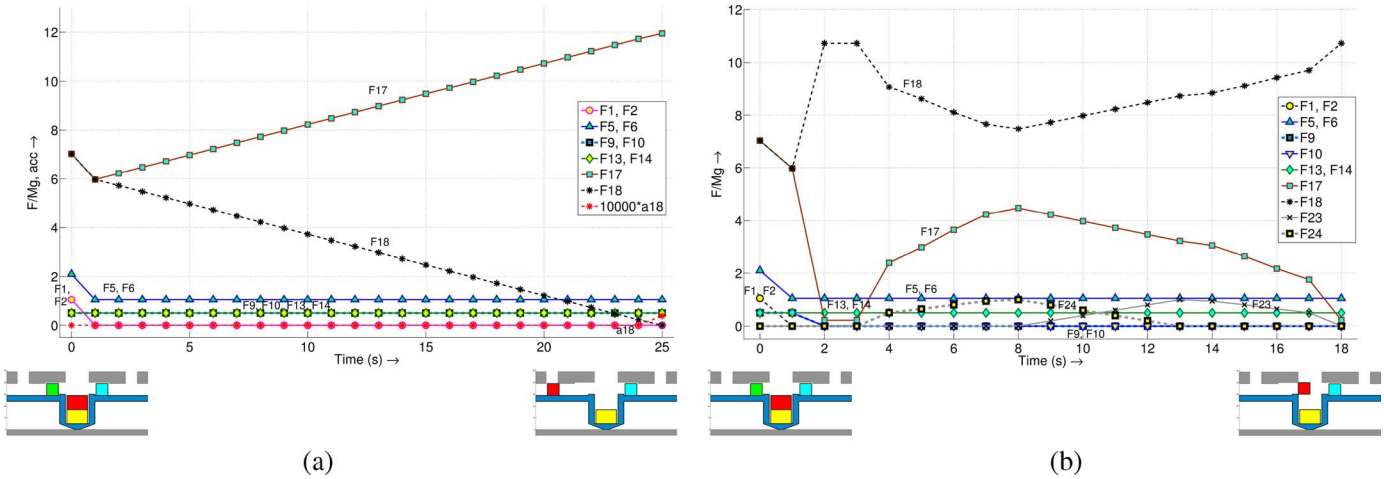

Fig. 8. Interplay of assembly sequence and motion paths. Y-axis shows the contact force normalized by the weight of C, and acceleration, and X-axis is time. (a) Block A is first moved out through center exit I. C is then moved to the left. At 25 s, before C is in position to exit through II, the assembly becomes unstable. Thus, when A is removed first, C cannot exit through either exit II or III. (b) A is moved out first and then C is moved to exit I. In this case the assembly remains stable.

TABLE I
STABILITY ANALYSIS RESULTS FOR DIFFERENT SEQUENCE AND MOTION PATH COMBINATIONS FOR THE ASSEMBLY OF FIG. 6. THE PATHS (INDICATED BY EXITS) FOR PARTS A, B, AND C ARE LISTED AS ORDERED TRIPLES IN THE ORDER OF THE SEQUENCE

Sequence	Path	Stable	Unstable
A-B-C	All		✓
A-C-B	(I, I, I)	✓	
A-C-B	(I, II, I), (I, III, I)		✓
C-A-B	(I, I, I), (II, I, I), (III, I, I)	✓	

II or III when A has been moved out. When C is lifted up and moved to the right towards exit I [Fig. 8(b)], C can be moved out through I at 18 s by the gripper [lower right hand figure of the assembly in Fig. 8(b)]. Thus when A is absent, C can be moved out stably only through exit I.

A similar analysis shows that removal of C after both A and B have been removed always leads to instability. We summarize the stability analysis results for sequence and motion path dependence in Table I. The motion path dependence for the disassembly of D is symmetric to that of C.

B. Influence of Motion Path in 3-D

We now consider a 3-D example to show that the LCP calculations for stability analysis can be extended to 3-D assemblies as well. Fig. 9(a) shows an assembly consisting of the frictionless blocks A, B, and C resting on a fixed support (table). Geometrically feasible disassembly paths exist for all the blocks. However, it is easy to see that if B is taken out first then both A and C will fall down. Hence, we only consider the disassembly sequences A-C-B and C-A-B for stability analysis. This example was solved using the LCPPATH solver [13].

When A is lifted up, the weight of C causes B to topple; this is manifested by positive accelerations at vertices 9 and 12 (Fig. 10). Thus, A-C-B is an unstable disassembly sequence. Next consider C-A-B. To illustrate the effect of motion path, we consider two paths for the removal of C, one along $+X$ and the other along the $-Y$ direction in Fig. 9(a). In both cases, the gripper supports the weight of C to the extent necessary to prevent C from falling down. Fig. 11 shows the normalized contact forces (with respect to the weight of C) when C is moved along the $-Y$ direction. Note that the contact forces at 9 and 10 increase and at 11 and 12 decrease as C is moved in the $-Y$ direction. At 12 s, the assembly becomes unstable and we see positive accelerations at 11 and 12.

Next consider moving C in the $+X$ direction. The support polygon 13–14–15–16 of the gripper prevents C from toppling as the downward projection of the centroid of C moves outside the contact polygon 5–6–7–8 [Fig. 12(b)]. The contact forces are shown in Fig. 13. There are no positive accelerations at the contact points, which implies stability. As C is moved in the $+X$ direction, the variation in load over B is manifested by the decrease in the contact forces at 9 and 12 and the increase in the contact forces at 10 and 11. The edge 13–16 of the support bears a higher fraction of the weight of C than the edge 14–15. The load on B through the edge 5–8 stays constant until the end (25 s) when edges 6–7 and 5–8 merge.

Thus we have shown using stability analysis that the disassembly sequence A-C-B is unstable under gravity, and the disassembly sequence C-A-B is path-dependent.

VI. CHARACTERIZATION OF MOTION PATH DEPENDENCE

To characterize motion path dependence, we establish conditions for stability and instability of frictionless disassembly problems. These provide a way to identify potential instability even without performing a stability analysis along the (dis)assembly paths. The results below are stated in the context of assembly stability as one part is removed. Let the part being grasped and moved by the gripper be P, the assembly including P be A, and the remainder of the assembly without P be $\overline{P}$, where $\overline{P} = A - P$.

Proposition 1: If $\overline{P}$ is unstable, then all motion paths for the disassembly of P from the assembly A are unstable.

Proof: All motion paths for disassembly of part P ultimately lead to the removal of P from assembly A. Irrespective

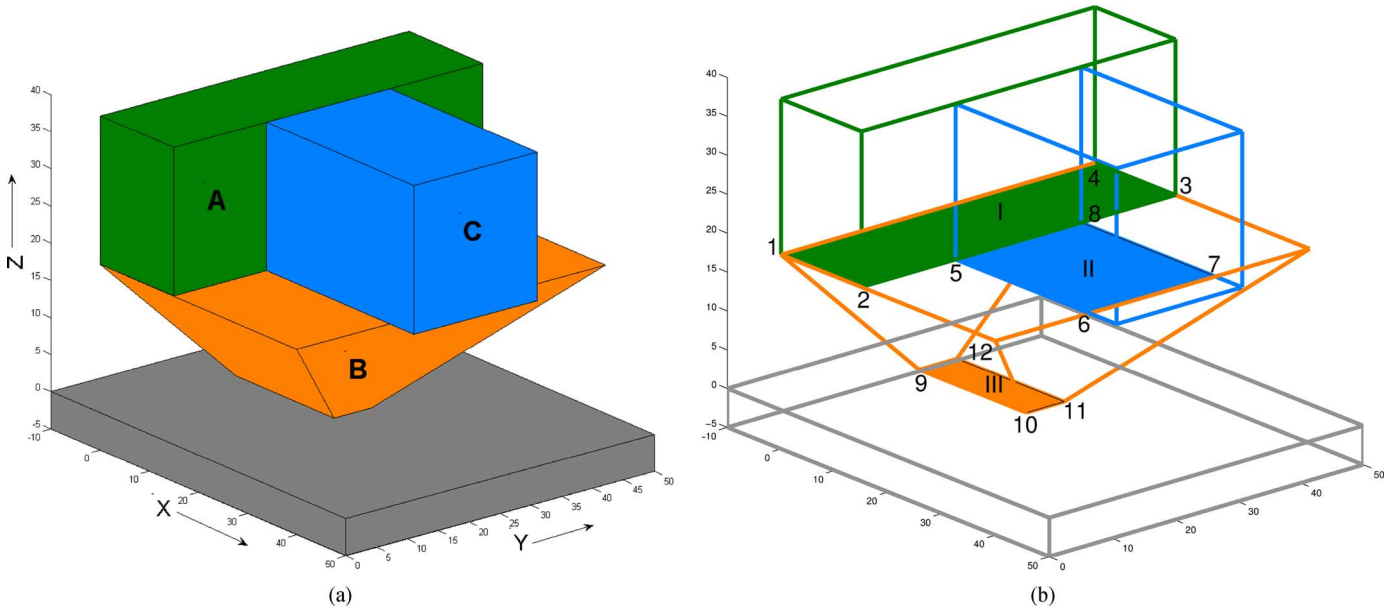

(a) (b)

Fig. 9. (a) Assembly consisting of frictionless blocks A, B, and C. (b) Wireframe view of A, B, and C showing the contact surfaces. The contact polygons between the blocks where contact forces occur are shown using different colors and numbered with Roman numerals. For example, the contact polygon between A and B is I with contact vertices 1, 2, 3, and 4.

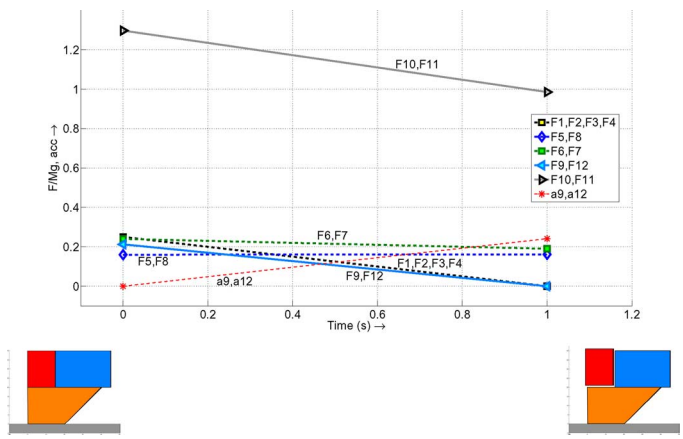

Fig. 10. A is lifted up from the assembly of Fig. 9. The contact forces are numbered according to the vertices of the contacting surfaces in Fig. 9(b). X-axis represents time. Y-axis represents the normalized contact forces with respect to the weight of A, and contact accelerations. When A is lifted up, positive accelerations at vertices 9 and 12 indicate the remaining assembly is unstable.

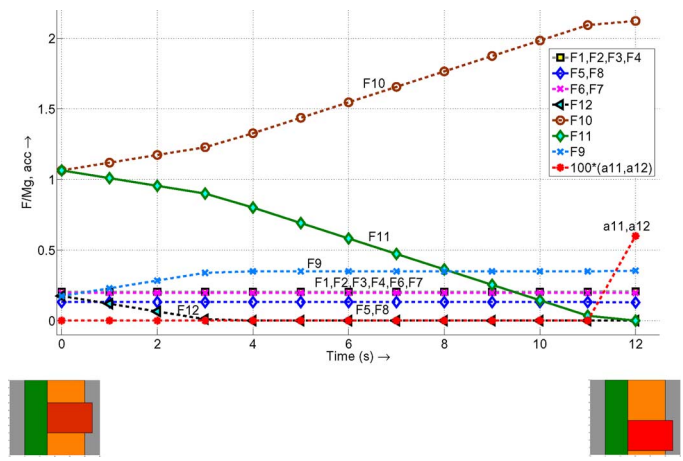

Fig. 11. Plot of the normalized contact forces and accelerations versus time when C is moved horizontally in the $-Y$ direction (Fig. 9(a)). The contact forces are normalized with respect to the weight of C. At 12 s the whole assembly becomes unstable and vertices 11 and 12 lose contact with the table. Accelerations at contact points 11 and 12 are shown magnified by a factor of 100. Top views of assembly shown at bottom.

of the motion path, the removal of P is equivalent to the detachment of P from assembly A. Hence, if detachment of a part from the assembly leads to instability, all motion paths will lead to instability. ■

Fig. 14 illustrates the proposition with an example.

Proposition 2: A sufficient condition for motion path independence in a disassembly problem is that the weight of the moving part is fully supported by the gripper.

Proof: Stability of an assembly depends on the contact forces between the mating parts. If the weight of part P is fully supported by the gripper, then P will not exert any contact force on $\overline{P}$ (under our assumptions in Section III-A). The situation is identical to the case when P is not part of A. Hence, motion paths cannot affect stability if the part's weight is fully supported by the gripper. ■

The contrapositive of Proposition 2 is that if the disassembly problem has path dependence, the moving part P is not fully supported by the gripper. Proposition 2 along with the fact that the gripper must fully support P when moving it vertically, leads to the following result.

Corollary 1: Part movement only in or opposite to the direction of gravity will not cause assembly instability due to the motion path.

We next identify conditions under which instability can occur when a part P is moved while not being fully supported by the gripper. (See Figs. 15 and 16 for stable and unstable examples.) We assume P is moving along a planar surface in the direction $\mathbf{m}$, and that the assembly A rests on a horizontal surface. We

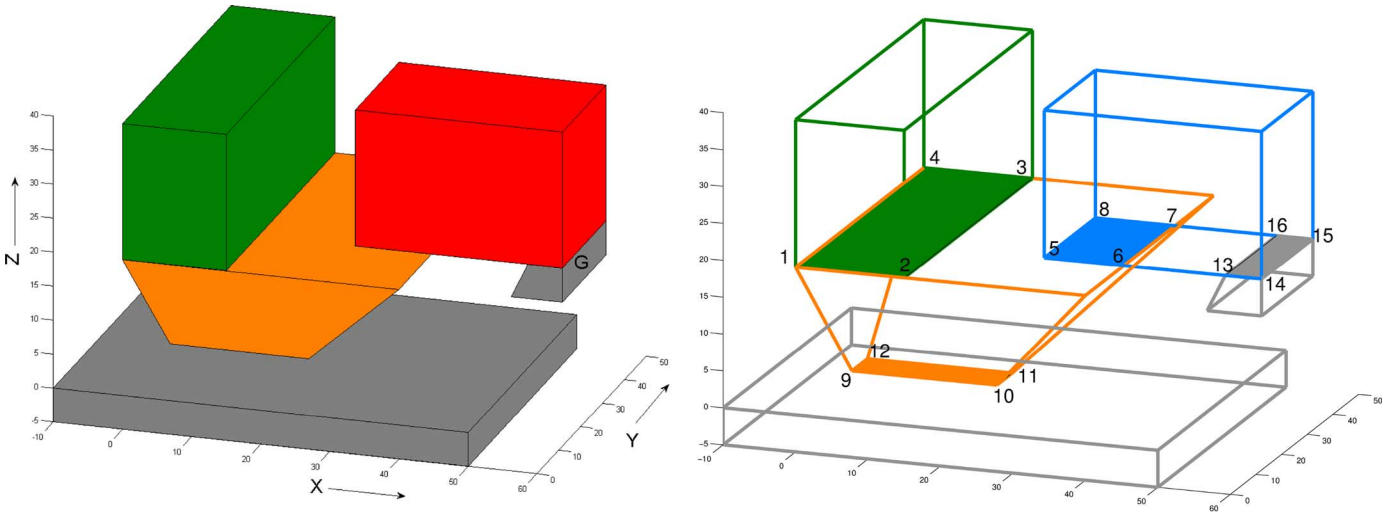

(a) (b)

Fig. 12. C is moved in $+X$ direction. To prevent toppling of C, the front end of C is supported by the gripper. (a) C in an intermediate position with the support of the gripper G at the leading end. (b) The wireframe diagram of the blocks with the contact polygons. The contact polygon between C and the gripper support is indicated by vertices 13, 14, 15, and 16.

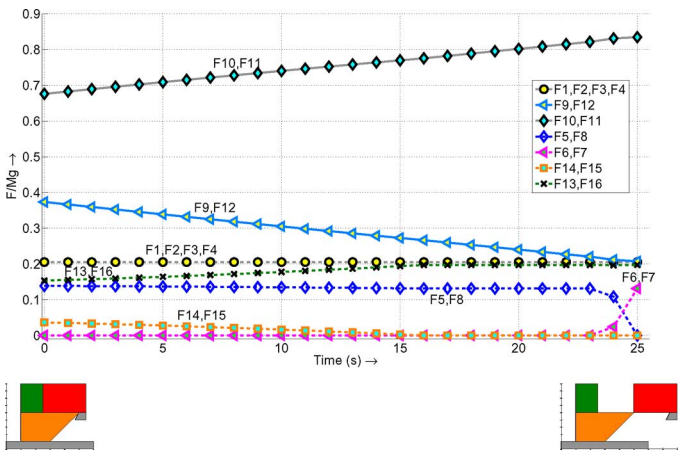

Fig. 13. Plot of the normalized contact forces versus time when C is supported by the gripper and moved in $+X$ direction. The contact forces are normalized with respect to the weight of C. The assembly stays stable throughout the motion path.

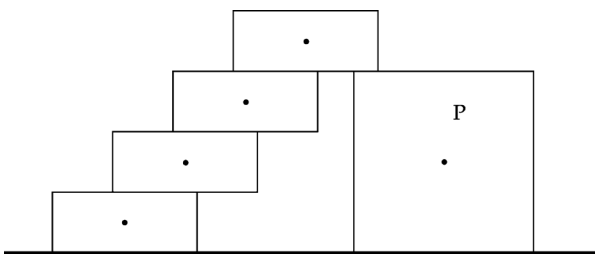

Fig. 14. Staircase of blocks supported by the block P under the topmost block. When P is moved out in any geometrically feasible direction from under the staircase, the staircase will no longer be stable.

also assume that the contact polygon has contiguous line contact (in the 2-D case) or surface contact (in the 3-D case) with the horizontal support surface. For polyhedral parts that are in contact with one another, the contact polygon is the boundary of the region of contact.

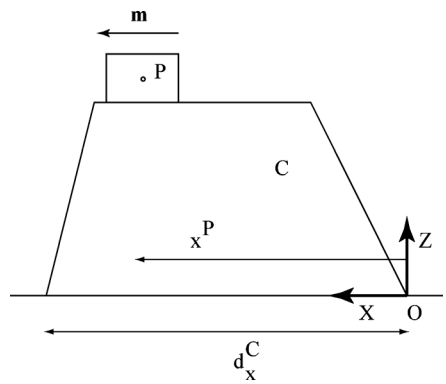

Fig. 15. Stable example. Part P can move along its support surface without the assembly becoming unstable.

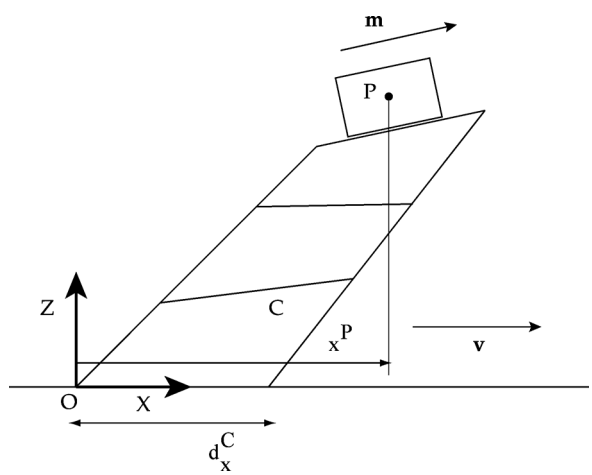

Fig. 16. Unstable example. Instability can occur when part P moves along a surface at a sufficiently large distance from a sufficiently narrow base of support.

Proposition 3: If the maximum distance x^P between the center of mass of P as it moves on its supporting planar surface and the vertices of the contact polygon on the horizontal table

along the projected motion direction is sufficiently larger than the maximum distance d_x^C between vertices of the contact polygon on the horizontal table along the projected motion direction, instability will occur.

Proof: Let the projection of the motion direction $\mathbf{m}$ on the horizontal table be the projected motion direction $\mathbf{v}$. We project the assembly on a plane $V_\perp$ perpendicular to the horizontal table and parallel to $\mathbf{v}$. In 2-D, $\mathbf{v}$ is parallel to the line representing the table, and $V_\perp$ is the plane in which the assembly lies. Let the part in contact with the table be C. Let $S_C = \{v_1, v_2, \ldots, v_K\}$ be the set of vertices of the contact polygon of C on the table. We locate the origin O at the vertex in S_C farthest from the centroid of P along $\mathbf{v}$, the X-axis along $\mathbf{v}$, the Z-axis along the upward normal to the table in the plane $V_\perp$, and the Y-axis by the right hand rule. So when P moves along $\mathbf{m}$, the moment due to the contact forces will only change about the Y-axis.

Let m^P be the mass of P and x^P be the X-coordinate of the center of mass (COM) of P. Let $m^{\overline{P}}$ be the mass of the remainder of the assembly $\overline{P}$ and $x^{\overline{P}}$ be the X-coordinate of the COM of $\overline{P}$. Let $\{x^{v_1}, x^{v_2}, \ldots, x^{v_K}\}$ be the X-coordinates of $\{v_1, v_2, \ldots, v_K\}$. Let $d_x^C = \max\{|x^{v_1}|, |x^{v_2}|, \ldots, |x^{v_K}|\}$. Let F_z be the net force along the Z-direction and M_y be the net moment along the Y-direction caused by the contact forces from the horizontal table. Considering equilibrium of forces along the Z-direction and moments along the Y-direction

$$m^P g + m^{\overline{P}} g = F_z = \sum_{i \in S_C} F_z^{v_i} \tag{6}$$

$$m^P g x^P + m^{\overline{P}} g x^{\overline{P}} = M_y = \sum_{i \in S_C} F_z^{v_i} x^{v_i}. \tag{7}$$

From (7), we can write

$$m^P g \frac{x^P}{d_x^C} + m^{\overline{P}} g \frac{x^{\overline{P}}}{d_x^C} = \frac{M_y}{d_x^C} = \sum_{i \in S_C} \frac{F_z^{v_i} x^{v_i}}{d_x^C} \leq \sum_{i \in S_C} F_z^{v_i}. \tag{8}$$

As P moves along $\mathbf{m}$, $m^{\overline{P}} g x^{\overline{P}}/d_x^C$ is constant while the magnitude of $m^P g x^P/d_x^C$ increases; the magnitude of M_y increases to maintain equilibrium. However, the maximum value that M_y/d_x^C can reach is F_z, which is constant for the assembly. If the polygonal surface on which P moves is such that the projected distance of its farthest vertex from the origin O along the X-direction is much larger than d_x^C, then P can move sufficiently far from O such that $x^P \gg d_x^C$, and (8) is no longer satisfied. This condition will lead to instability. ■

We now illustrate the above proposition with respect to the presented 2-D and 3-D examples. In the 2-D example (Fig. 6), the horizontal projection of the base is the length of the edge between vertices 17 and 18, which is smaller than the horizontal projection of the top surface over which C moves. Hence, the moment arm of C can be much larger than the moment arm of the contact forces from the horizontal table, i.e., the length of the edge 17–18. The instability (Fig. 7) is induced by the increasing moment as C moves to the left. The increasing moment eventually makes the contact force decrease to zero at vertex 18, after which instability is induced.

In the 3D example, note that the horizontal projection of the base along the motion direction along the negative Y-axis (the edge 10–11 in Fig. 9), is smaller than the horizontal projection of the top surface of B along the same direction (edge 2–3). In this case, when C is moved in the $-Y$ direction, the instability is induced due to the increasing difference between contact forces at {9,10} and {11,12} to counterbalance the moment due to the weight of C. Note that if the weight of P is fully supported by the gripper, then $m^P g x^P/d_x^C$ is zero in (8), and the equations of static equilibrium are satisfied for all paths, consistent with Proposition 2.

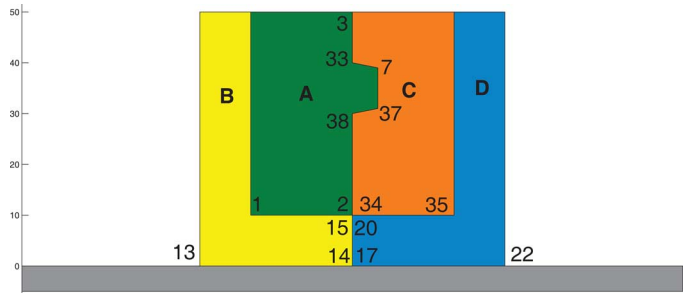

Fig. 17. Example for disassembly of subassemblies. Frictionless blocks A, B, C, and D rest on a fixed support. The vertices relevant for the contact forces are shown. As removal of individual parts leads to instability, {A-B, C-D} is the only stable subassembly sequence for disassembly.

We use linear complementarity to perform stability analysis at discrete configurations as parts are moved out of the assembly. We ask the question: Given that at two discrete configurations the assembly is stable, when can we guarantee that the assembly is stable for all configurations between those two configurations? We prove that if disassembly is *path independent* as defined in Section V (for example, when the part is supported by the gripper), the assembly will be stable at all configurations between a pair of stable start and end configurations.

Proposition 4: For path-independent disassembly, if the assembly A at any two configurations of a path is stable as part P is moved, then it is stable at all configurations along the path between the two configurations.

Proof: Let i, j, and k be three different configurations of the assembly A along a path for P, with k being an intermediate configuration between i and j as P is moved out. Let V_P^q and $V_{\overline{P}}^q$ denote the potential energy of P and $\overline{P}$ respectively at a configuration q. Let i and j be stable configurations, and assume the intermediate configuration k is unstable. This implies that at configuration k, some part(s) in $\overline{P}$ will begin to move and gain kinetic energy. Since the gripper does work on only P by our assumptions, the gain in kinetic energy of part(s) in $\overline{P}$ will lead to a decrease in potential energy of $\overline{P}$ at k, i.e., $V_{\overline{P}}^k$. The parts at the configuration k that are not in equilibrium will move to new equilibrium states with lower potential energy. Since all parts other than P are in their unchanged locations at configurations i and j, therefore $V_{\overline{P}}^i = V_{\overline{P}}^j > V_{\overline{P}}^k$. However the gripper does work only on P, and hence it cannot do work and increase the potential energy of the parts that have moved into lower potential energy states. Hence, for all configurations at and after k on the path, the potential energy of $\overline{P}$ will be less than or equal to $V_{\overline{P}}^k$. Since j lies after k, therefore, $V_{\overline{P}}^k \geq V_{\overline{P}}^j$. But this directly contradicts our assumption that $V_{\overline{P}}^k < V_{\overline{P}}^i = V_{\overline{P}}^j$. Therefore k must be a stable configuration. ■

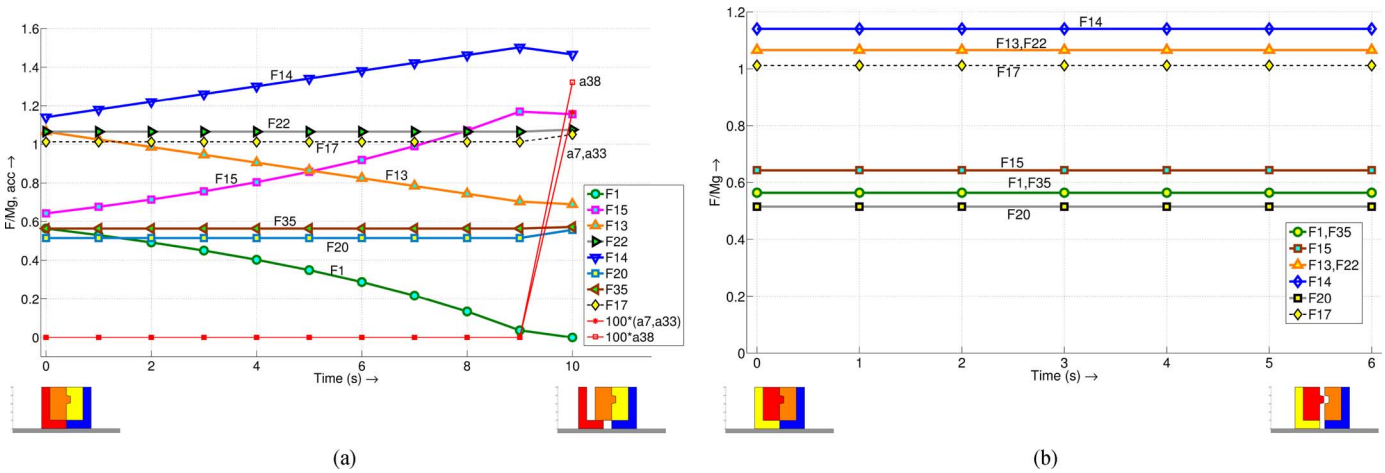

(a) (b)

Fig. 18. Plot of normalized force versus time for disassembly of the assembly of Fig. 17. All forces are normalized with respect to the weight of A. (a) B is moved to the left. At 10 s, A becomes unstable, as shown by positive accelerations at contact points 7, 33 and 38. (b) Subassembly A-B is moved to the left. The gripper grasps and moves A, which pushes B to the left. The disassembly is stable.

Corollary 2: For the case of path-independent disassembly, checking for stability at the nodes of the AND/OR graph of the disassembly tree is sufficient to verify stable disassembly sequences.

Proof: For path-independent disassembly, it follows from Proposition 4 that if the two configurations that correspond to the state of the assembly with and without the part P respectively are stable, then $\overline{P}$ will be stable at all configurations while P is being disassembled. Thus for the case of path-independent disassembly, checking stability at the nodes of the AND/OR graph of the disassembly tree is sufficient to verify stable disassembly sequences. ■

VII. Disassembly of Subassemblies

So far we have applied stability analysis to the case of single part disassembly. However, the efficiency of disassembly can be increased by simultaneous disassembly of multiple parts as subassemblies. In some cases, disassembly of subassemblies may be the only stable disassembly process. We present an example to illustrate that stability analysis can also help in selection of stable subassemblies. Fig. 17 shows four blocks A, B, C, and D forming an assembly. There is no friction between the blocks, and between the blocks and the support. For two handed disassembly, the possible subassemblies for disassembly are: {A-B, C-D}, {A-B-C, D}, {A-C-D, B}, and {A-C, B-D}. Removal of any single part from the assembly results in instability. A or C cannot be lifted up independently without causing instability, and have to be held together and lifted simultaneously for stable disassembly. B and D can be moved sideways, but the motion of either leads to instability. Fig. 18(a) shows the contact forces and the accelerations leading to instability when B is moved to the left by the gripper. After B has moved to the left, at 10 s, A becomes unstable [shown by contact accelerations at vertices 7, 33 and 38 in Fig. 18(a)].

On the other hand, when A is moved to the left, it pushes B along with it, and the disassembly is stable. The contact forces are shown in Fig. 18(b). A can then be stably disassembled from B, and similarly C can be stably disassembled from D. Thus, the stable disassembly of the example shown in Fig. 17 can only be executed by considering subassemblies.

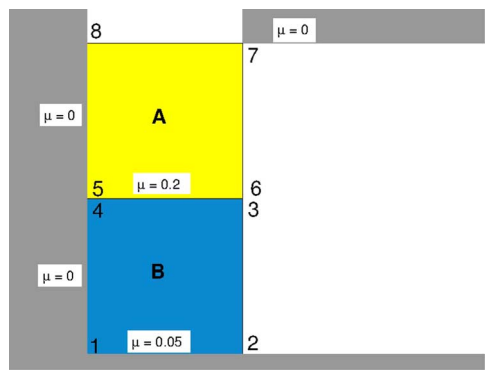

Fig. 19. Noninvertible disassembly example. The blocks can be disassembled either by lifting from the top (invertibly) or by moving horizontally (noninvertibly). The friction coefficients between different surfaces are shown.

VIII. Noninvertibility of Assembly and Disassembly

When only geometric constraints are considered, a two-handed monotone disassembly can be inverted for assembly [17]. However, when physical forces are considered, a two-handed monotone assembly and disassembly might not be invertible. Although this has been previously noted [20], [17], we are not aware of a prior exploration of this issue based on simulation. We construct a simple example to illustrate how a physical force, i.e., friction, may lead to noninvertibility of assembly and disassembly. The assembly consists of two rigid blocks A and B (Fig. 19) that can be disassembled either by moving vertically, or by moving horizontally. The disassembly sequence is A-B, and the assembly sequence is B-A. In the vertical direction, assembly and disassembly are invertible.

Let us now consider disassembly when A is moved out to the right. We select the coefficients of friction between different surfaces as shown in Fig. 19, that is, μ is 0.2 between A and B, 0.05 between B and its support surface, and zero between all other surfaces. The weight of each block is one unit. The complementarity conditions for this system are given by (5), and we use the

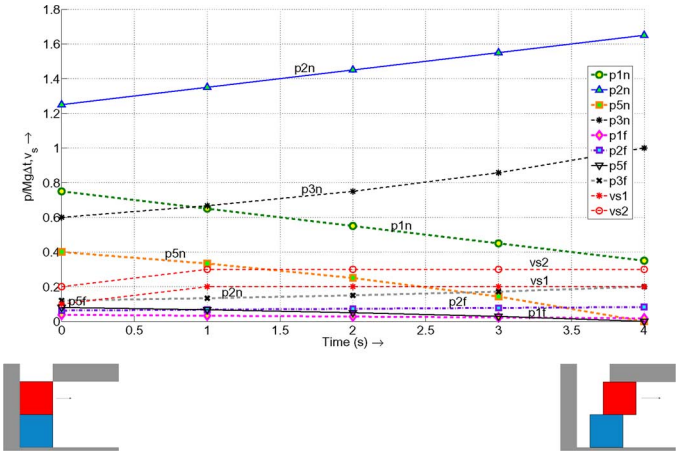

Fig. 20. Plot of normal contact and friction impulses when A is moved to the right, normalized by the normal impulse of A. The subscripts n and f indicate the normal contact impulses and friction impulses. The sliding velocity between A and B is vs_2 and that between B and the base is vs_1.

LCPPATH solver to calculate the forces between different parts in the assembly (Fig. 20). When a force high enough to move A to the right is applied, it begins to slide and drags B along with it due to imbalance of friction forces between the top and bottom surfaces of B. Since movement of A induces movement in B, the disassembly sequence is unstable. If we invert this disassembly sequence, then the assembly sequence is B-A. When A is inserted horizontally over B from the right, the sliding motion of B is prevented by the left wall, and hence it is stable. Thus, when the horizontal path is selected, assembly B-A and disassembly A-B are not invertible.

IX. Conclusion

The focus of this paper is the influence of part motion and assembly sequence on assembly stability. Given this goal, we go beyond the prior approach of performing a static analysis of the disassembly tree. We instead use linear complementarity to perform the stability analysis at each step of motion in the disassembly process as parts are removed sequentially. We showed that disassembly sequences that are consistent with only geometric contraints may be infeasible in the presence of gravity or friction. Furthermore, stability analysis can be used to identify and prevent instability inducing motions by introducing fixtures, by selecting alternative motion paths, or by alternative disassembly sequences. Previously, only the disassembly sequence had been shown to be important for stable disassembly. We have shown that not only the disassembly sequence, but the motion paths of the parts also can affect the stability of the disassembly process. We explored the interplay of motion path and sequence for both 2-D and 3-D examples. We further proved conditions for motion path dependence in disassembly problems. We additionally proved that our LCP based stability analysis and the prior AND/OR graph based static stability analysis [25] yield the same result for path-independent disassemblies. We then extended stability analysis of single part disassembly to stability analysis of subassemblies. We also showed that assembly and disassembly, invertible when only geometric constraints are considered, can become noninvertible in the presence of friction.

Acknowledgment

The authors would like to thank N. Chakraborty, R. Mattikalli, and J. Trinkle for informative discussions and J. Williams for technical assistance.

References

[1] D. Baraff, "Analytical methods for dynamic simulation of nonpenetrating rigid bodies," *ACM SIGGRAPH Comput. Graph.*, vol. 23, no. 3, pp. 223–232, 1989.
[2] D. Baraff, "Fast contact force computation for nonpenetrating rigid bodies," in *Proc. Annu. Conf. Comput. Graph. and Interactive Techn.*, 1994, pp. 23–34.
[3] D. Baraff, R. Mattikalli, and P. Khosla, "Minimal fixturing of frictionless assemblies: Complexity and algorithms," *Algorithmica*, vol. 19, no. 1/2, pp. 4–39, 1997.
[4] J. D. Bernheisel and K. M. Lynch, "Stable transport of assemblies: Pushing stacked parts," *IEEE Trans. Automat. Sci. Eng.*, vol. 1, no. 2, pp. 163–168, Oct. 2004.
[5] J. D. Bernheisel and K. M. Lynch, "Stable transport of assemblies by pushing," *IEEE Trans. Robot.*, vol. 22, no. 4, pp. 740–750, Aug. 2006.
[6] M. Blum, A. Griffith, and B. Neumann, "A stability test for configurations of blocks," Mass. Inst. Technol., Tech. Rep. AI Memo. 188, 1970.
[7] N. Boneschanscher, H. van der Drift, S. J. Buckley, and R. H. Taylor, "Subassembly stability," in *Proc. Nat. Conf. Artif. Intell.*, 1988, pp. 780–785.
[8] G. Boothroyd and P. Dewhurst, *Assembly Automation and Product Design*. New York, NY, USA: Taylor and Francis, 2005.
[9] R. C. Brost and K. Y. Goldberg, "A complete algorithm for designing planar fixtures using modular components," *IEEE Trans. Robot. Automat.*, vol. 12, no. 1, pp. 31–46, Feb. 1996.
[10] R. C. Brost and R. R. Peters, "Automatic design of 3-D fixtures and assembly pallets," *Int. J. Robot. Res.*, vol. 17, no. 12, pp. 1243–1281, Dec. 1998.
[11] R. W. Cottle, J. S. Pang, and R. E. Stone, *The Linear Complementarity Problem*. Boston, MA, USA: Academic, 1992.
[12] L. S. H. de Mello and A. C. Sanderson, "AND/OR graph representation of assembly plans," *IEEE Trans. Robot. Automat.*, vol. 6, no. 2, pp. 188–199, Apr. 1990.
[13] S. P. Dirkse and M. C. Ferris, "The PATH solver: A non-monotone stabilization scheme for mixed complementarity problems," *Optimizat. Methods and Software*, vol. 5, pp. 123–156, 1995.
[14] E. Ferré and J. P. Laumond, "An iterative diffusion algorithm for part disassembly," in *Proc. IEEE Int. Conf. Robot. Automat.*, New Orleans, LA, USA, Apr. 2004, pp. 3149–3154.
[15] K. Y. Goldberg and H. Moradi, "Compiling assembly plans into hard automation," in *Proc. IEEE Int. Conf. Robot. Automat.*, Minneapolis, MN, USA, Apr. 1996, pp. 1858–1863.
[16] D. Halperin, L. Kavraki, and J.-C. Latombe, "Robotics," in *Handbook of Discrete and Computational Geometry*, J. E. Goodman and J. O'Rourke, Eds., 2nd ed. Boca Raton, FL, USA: Chapman and Hall/CRC, 2004, pp. 1065–1093.
[17] D. Halperin, J. C. Latombe, and R. H. Wilson, "A general framework for assembly planning: The motion space approach," *Algorithmica*, vol. 26, no. 3–4, pp. 577–601, 2000.
[18] A. J. D. Lambert and S. M. Gupta, *Disassembly Modeling for Assembly, Maintenance, Reuse, and Recycling*. Boca Raton, FL, USA: CRC, 2005.
[19] D. T. Le, J. Cortes, and T. Simeon, "A path planning approach to (dis)assembly sequencing," in *Proc. IEEE Int. Conf. Automat. Sci. Eng.*, Bangalore, India, Aug. 2009, pp. 286–291.
[20] S. Lee and H. Moradi, "Disassembly sequencing and assembly sequence verification using force flow networks," in *Proc. IEEE Int. Conf. on Robot. Automat.*, Detroit, MI, USA, May 1999, pp. 2762–2767.
[21] M. T. Mason, *Mechanics of Robotic Manipulation*. Cambridge, MA, USA: MIT, 2001.
[22] R. Mattikalli, D. Baraff, and P. Khosla, "Finding all stable orientations of assemblies with friction," *IEEE Trans. Robot. Automat.*, vol. 12, no. 2, pp. 290–301, Apr. 1996.
[23] R. Mattikalli, D. Baraff, P. Khosla, and B. Repetto, "Gravitational stability of frictionless assemblies," *IEEE Trans. Robot. Automat.*, vol. 11, no. 3, pp. 374–388, Jun. 1995.
[24] H. Mosemann, F. Rohrdanz, and F. M. Wahl, "Stability analysis of assemblies considering friction," *IEEE Trans. Robot. Automat.*, vol. 13, no. 6, pp. 805–813, Dec. 1997.

[25] H. Mosemann, F. Rohrdanz, and F. M. Wahl, "Assembly stability as a constraint for assembly sequence planning," in *Proc. IEEE Int. Conf. Robot. Automat.*, Leuven, Belgium, May 1998, pp. 233–238.
[26] R. M. Murray, Z. Li, and S. S. Sastry, *A Mathematical Introduction to Robotic Manipulation*. Boca Raton, FL, USA: CRC, 1994.
[27] R. S. Palmer, "Computational complexity of motion and stability of polygons," Ph.D. dissertation, Dept. Comput. Sci., Cornell Univ., Ithaca, NY, USA, 1987.
[28] J. S. Pang and J. C. Trinkle, "Stability characterizations of fixtured rigid bodies with Coulomb friction," in *Proc. IEEE Int. Conf. Robot. Automat.*, San Francisco, CA, USA, Apr. 2000, pp. 361–368.
[29] S. Rakshit and S. Akella, "The influence of sequence and motion path on the stability of assemblies," in *Proc. Robot.: Sci. Syst. Conf.*, Berlin, Germany, Jun. 2013.
[30] B. Romney, "Atlas: An automatic assembly sequencing and fixturing system," in *Proc. Int. Conf. Theory and Practice of Geometric Modeling*, 1997, pp. 397–415.
[31] D. E. Stewart and J. C. Trinkle, "An implicit time-stepping scheme for rigid body dynamics with inelastic collisions and Coulomb friction," *Int. J. Numer. Methods Eng.*, vol. 39, pp. 2673–2691, 1996.
[32] S. Sundaram, I. Remmler, and N. M. Amato, "Disassembly sequencing using a motion planning approach," in *Proc. IEEE Int. Conf. Robot. Automat.*, Seoul, Korea, May 2001, pp. 1475–1480.
[33] J. C. Trinkle, "On the stability and instantaneous velocity of grasped frictionless objects," *IEEE Trans. Robot. Automat.*, vol. 8, no. 5, pp. 560–572, Oct. 1992.
[34] J. Wang, P. Rogers, L. Parker, D. Brooks, and M. Stilman, "Robot Jenga: Autonomous and strategic block extraction," in *Proc. IEEE/RSJ Int. Conf. Intell. Robots Syst.*, St. Louis, MO, USA, Oct. 2009, pp. 5248–5253.
[35] D. E. Whitney, *Mechanical Assemblies: Their Design, Manufacture, and Role in Product Development*. New York, NY, USA: Oxford Univ., 2004.
[36] R. H. Wilson and J.-C. Latombe, "Geometric reasoning about mechanical assembly," *Artif. Intell.*, vol. 71, no. 2, pp. 371–396, Dec. 1994.
[37] J. D. Wolter and J. C. Trinkle, "Automatic selection of fixture points for frictionless assemblies," in *Proc. IEEE Int. Conf. Robot. Automat.*, San Diego, CA, USA, May 1994, vol. 1, pp. 528–534.

Sourav Rakshit received the B.E. degree from Jadavpur University, Kolkata, India, in 1999, and the M.E. and Ph.D. degrees from the Indian Institute of Science, Bangalore, India, in 2006 and 2012, respectively, all in mechanical engineering.

He was a Scientific Officer with Bhabha Atomic Research Centre (BARC), India, from 1999 to 2004, and a Postdoctoral Researcher with the University of North Carolina at Charlotte, Charlotte, NC, USA, from 2012 to 2014. He is currently an Assistant Professor with the Indian Institute of Technology, Madras, India. His current research interests include multibody mechanics, biomechanics, assembly planning, robotics, and optimization algorithms.

Srinivas Akella (S'90–M'00) received the B.Tech. degree from the Indian Institute of Technology, Madras, India, in 1989, and the Ph.D. degree in robotics from Carnegie Mellon University, Pittsburgh, CA, USA, in 1996.

He is currently a Faculty Member with the Department of Computer Science, University of North Carolina at Charlotte, Charlotte, NC, USA. He was previously on the faculty of the Computer Science Department, Rensselaer Polytechnic Institute, Troy, NY, USA, and was a Beckman Fellow with the Beckman Institute, University of Illinois at Urbana-Champaign, Urbana, IL, USA, prior to that. His research interests are in developing geometric and optimization algorithms for robotics, automation, and biotechnology applications.

Dr. Akella was a recipient of the National Talent Search Scholarship from the Government of India and the National Science Foundation CAREER Award.